

# A matrix-based method for the structural analysis of diagrid systems

Giuseppe Lacidogna\*, Domenico Scaramozzino, Alberto Carpinteri

Department of Structural, Geotechnical and Building Engineering, Politecnico di Torino, Corso Duca degli Abruzzi 24, 10129 Torino, Italy

## ARTICLE INFO

### Keywords:

Diagrid structural system  
Matrix-based method  
Tall buildings  
Stiffness matrix  
Lateral displacement  
Swiss Re Tower  
General Algorithm  
Distribution matrix

## ABSTRACT

Diagrid systems have been frequently employed in the last few decades for the construction of tall buildings because of their high lateral stiffness and for their capability to realize complex-shaped structures. Considering mainly diagrid structures with regular forms, many researchers have developed different methods to perform the structural analysis. In this paper, a matrix-based method (MBM) for the analysis of generic freeform diagrid systems is proposed. Unlike existing methodologies, that take into account only shear and bending stiffness, and Finite Element Method approach, the proposed procedure is based on the direct calculation of the complete structure stiffness matrix, without the assemblage of local sub-matrices. This method allows to solve automatically the structural problem, providing both the structure displacements and the axial forces in the diagonals. Then, some comparisons with the Finite Element Method are reported, both for two-dimensional and three-dimensional diagrid systems. In order to show the method capabilities, the analysis concerning the Swiss Re Tower in London is performed. Finally, an application of the MBM is shown regarding the distribution of lateral actions between an external diagrid system and a central core, according to the General Algorithm theory.

## 1. Introduction

Leaving aside the history of the origins, the modern tall buildings began to be built mainly in the United States at the beginning of the 20th century. Originally they were made up of spatial frames coupled with vertical shear walls, designed as vertical cantilevers, and allowed to reach a few hundred metres heights. With the escalation of the height development demand, the adoption of new structural systems was needed, because of the increasing importance of lateral actions such as wind or earthquake loads. Therefore, in the following decades, new typologies of tall buildings were developed, such as framed tube and tube-in-tube systems [1,2]. These typologies exploited the mechanical properties of external tubular structural elements to withstand lateral actions and reduce lateral displacements.

At the end of the 20th century and especially during the first decade of the 21st century, tall buildings began to be conceived and realized also in other countries, particularly in Asia, i.e. in China, Malaysia, Saudi Arabia and United Arab Emirates. Together with this geographical shift, new kinds of systems appeared, such as tapered and twisted structures, which allowed to increase both the structural performance and architectural impact. Finally, combining both the need to improve the structural behaviour and to realize complex-shaped impressive tall buildings, the first diagrid (*diagonal + grid*) systems were realized [3–5]. One of the first steps which led to the realization of

diagrid systems was the introduction of bracing members on the outside of typical framed structures, in addition to horizontal beams and vertical columns, as in the case of the John Hancock Center (Chicago). In order to resist lateral forces, the more the height of the building, the more the importance of these additional structural elements.

After a few decades, it was understood that diagonal members could be exploited not only to withstand lateral actions, but also to carry vertical loads, making the conventional columns no longer necessary. The mega-diagonals, which could extend for several floors, were set all over the exterior of the building, also increasing the aesthetic potential of the structure. This new kind of structure provided remarkable performance in terms of stiffness, exploiting the axial resisting mechanism of inclined diagonals instead of the bending behaviour of conventional vertical columns. Because of the versatility of diagonals, diagrid systems allowed to realize impressive complex-shaped tall buildings, as shown in Fig. 1. In fact, diagrid structures being composed by the assembly of elementary members (i.e. the single diagonals), the geometric pattern could be changed until the desired structural shape was reached. Therefore, as in the case of Swiss Re Tower in London (Fig. 1a) and Tornado Tower in Doha (Fig. 1b), double-curvature structures could be realized, achieving remarkable architectural effects. Moreover, freeform diagrid buildings could be obtained too, as shown by the Capital Gate in Abu Dhabi (Fig. 1c).

Even though this kind of structural system was quite new, many

\* Corresponding author.

E-mail address: [giuseppe.lacidogna@polito.it](mailto:giuseppe.lacidogna@polito.it) (G. Lacidogna).



**Fig. 1.** Examples of diagrid structural systems: (a) Swiss Re Tower, London (from <http://larryspeck.com>); (b) Tornado Tower, Doha (from <http://www.asergeev.com>); (c) Capital Gate, Abu Dhabi (from <https://www.rmjm.com>).

researchers focused their attention on the development of different methodologies for the analysis and design of diagrid systems. All of them started from the same main assumptions: the only resisting mechanism is offered by the presence of the diagonals, which are assumed to be only subject to axial force; the floors remain plane after the deformation of the structure; the floors included within the modules of the mega-diagonals are neglected regarding the global behaviour of the structure. Initially, the studies were performed by Moon *et al.* [6] on the analysis of simple buildings with rectangular plans, vertical façades, and constant inclination angles of the diagonals. An analytical method, based on the calculation of shear and bending stiffness of the modules, was developed for the determination of the optimal diagonal angle and to provide a procedure able to preliminary compute the structural elements dimensions [6]. Starting from these fundamental considerations, several researches enriched the studies about the subject: twisted, tilted and freeform diagrid towers were analysed through Finite Element Method [7]; diagrid systems with gradually varying angles, or with changing density patterns, were subjected to the process of the optimal angles determination [8–11]; double-curvature structures were studied with a suggested hand calculation, and some comparisons with FEM analysis were proposed regarding real buildings [12]. More recently, Liu and Ma (2017) developed a modular method, based on the calculation of modular lateral stiffness, which allowed to solve the structural problem for arbitrary polygonal diagrid systems having vertical façades or with a constant inclination [13].

In this paper, a matrix-based method (MBM) for the structural analysis of freeform diagrid systems, based on the calculation of the structure stiffness matrix, is proposed. The calculation of the stiffness coefficients is presented considering the same assumptions reported in [6–13]. Initially, the procedure for the analysis of two-dimensional diagrid systems is introduced, considering two degrees of freedom per floor. Afterwards, the same procedure is applied to generic three-dimensional diagrid systems, becoming useful for the calculation of more complex spatial structures. Eventually, to show the method capabilities, the analysis of Swiss Re Tower (Fig. 1a) is performed [14].

As shown in Section 4 concerning the analysis of three-dimensional

structures, MBM takes into account six degrees of freedom per floor; therefore, by applying it, useful information can be obtained not only regarding horizontal and vertical floor displacements, but also regarding out-of-plane and in-plane floor rotations, due respectively to horizontal actions and torque moments. Therefore, MBM can provide significant information about vertical and lateral deformability of the structure as well as regarding torsional behaviour. Moreover, in order to study the problem of the distribution of lateral actions between several elements, such as shear wall-frames or thin-walled closed and open sections within a three-dimensional complex building, the application of the MBM within the so called General Algorithm, firstly proposed by A. Carpinteri and An. Carpinteri in 1985 [15] and further developed in [16–21], is discussed. Finally, an example is proposed, in order to evaluate the distribution of lateral actions between an external diagrid system and a central core.

## 2. The procedure for the calculation of the structure stiffness matrix

As mentioned in the Introduction, MBM is based on the direct calculation of the stiffness matrix of diagrid structural systems. Despite being founded on matrix analysis, it differs substantially from the Finite Element Method. As is well known, FEM starts from the formulation of the stiffness matrices of single elements, which are then expanded to the structure dimension and assembled to obtain the global structure stiffness matrix taking into account constraint conditions.

In this case, the structural problem is formulated through a matrix relation, which allows to link the vector of external forces acting on the structure to the vector of floor displacements, through the global stiffness matrix of the structure. The inputs are the forces (and moments) acting on the floors of the structure, the outputs are the unknown displacements (and rotations) of the floors. The main hypotheses are the same considered by other authors whose approach is explained in [6–13]: diagonals, having linear elastic behaviour, are only subject to axial force; floors remain plane after the deformation of the structure, so that they can be considered as rigid bodies in the space,

characterized by a low number of degrees of freedom; the floors included within the modules of diagonals are neglected.

The stiffness matrix of the structure is computed through the following observation concerning the matrix coefficients: each coefficient  $k_{ij}$  represents the total floor reaction force (or moment) on the  $i$ th floor, produced by an imposed unitary floor displacement (or rotation) on the  $j$ th floor. Applying this procedure to the whole structure and considering the abovementioned hypotheses, the stiffness matrix of the structure can be totally computed, providing the solution of the structural problem. This procedure (applied both for two-dimensional and three-dimensional systems) has been implemented into the MatLab code, in order to allow an automatic calculation of the structural problem. Therefore, given the information about the diagrid structure and the external acting forces, the suggested model allows to compute automatically the diagrid stiffness matrix, the displacements (and the rotations) of the floors and the diagonal axial forces.

### 3. Analysis of two-dimensional diagrid systems

First of all, the analysis of two-dimensional diagrid structural systems is presented, mainly in order to show the MBM fundamental concepts. A diagrid structure is considered, which is generally made up of  $M$  floors and  $N$  modules of diagonals (with  $M \geq N$ ), both conventionally numbered from the top to the bottom of the system, within a two-dimensional space characterized by an XY reference system (Fig. 2). As shown in Fig. 2, the floors included within the modules are neglected in the present analysis; therefore, only the  $N$  floors at the ends of the diagonals are considered. For sake of clarity, in the remaining of the text, the word “floors” will be referred just to the ones actually considered in the present analysis. Moreover, they are assumed continue and infinitely rigid in-plane, whereas diagonals are simply hinged.

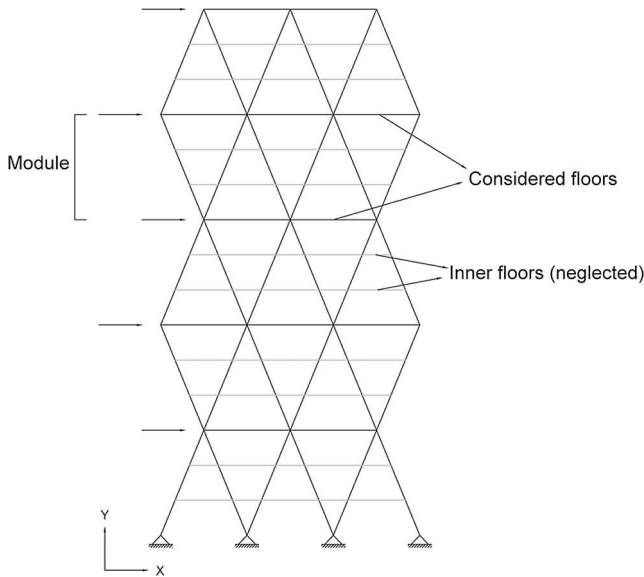


Fig. 2. Two-dimensional diagrid structural system.

#### 3.1. Two-degree-of-freedom per floor model

The structure is subjected to horizontal forces and the hypothesis of two degrees of freedom per floor (i.e. horizontal displacement and out-of-plane rotation) is considered. The structural problem can be formulated through a matrix relation as follows:

$$\begin{Bmatrix} \{F\} \\ \{M\} \end{Bmatrix} = \begin{bmatrix} [K_{F\delta}] & [K_{F\varphi}] \\ [K_{M\delta}] & [K_{M\varphi}] \end{bmatrix} \begin{Bmatrix} \{\delta\} \\ \{\varphi\} \end{Bmatrix}, \quad (1)$$

where  $\{F\}$  and  $\{M\}$  are the  $N$ -vectors containing respectively the  $N$  floor forces and moments,  $\{\delta\}$  and  $\{\varphi\}$  are the  $N$ -vectors containing the unknown floor displacements and rotations,  $[K_{F\delta}]$  is the  $N \times N$  stiffness matrix which relates the floor forces to the floor displacements,  $[K_{M\varphi}]$  is the  $N \times N$  stiffness matrix which relates the floor moments to the floor rotations,  $[K_{F\varphi}]$  is the  $N \times N$  stiffness matrix which relates the floor forces to the floor rotations, and  $[K_{M\delta}]$  is the  $N \times N$  stiffness matrix which relates the floor moments to the floor displacements.

Eq. (1) can be rewritten, by specifying the terms included within the force and displacement vectors and the structure stiffness matrix:

$$\begin{Bmatrix} F_1 \\ \vdots \\ F_i \\ \vdots \\ F_N \\ M_1 \\ \vdots \\ M_i \\ \vdots \\ M_N \end{Bmatrix} = \begin{bmatrix} k_{11}^{F\delta} & \dots & k_{1i}^{F\delta} & \dots & k_{1N}^{F\delta} & k_{11}^{F\varphi} & \dots & k_{1i}^{F\varphi} & \dots & k_{1N}^{F\varphi} \\ \vdots & \vdots & \vdots & \vdots & \vdots & \vdots & \vdots & \vdots & \vdots & \vdots \\ k_{i1}^{F\delta} & \dots & k_{ii}^{F\delta} & \dots & k_{iN}^{F\delta} & k_{i1}^{F\varphi} & \dots & k_{ii}^{F\varphi} & \dots & k_{iN}^{F\varphi} \\ \vdots & \vdots & \vdots & \vdots & \vdots & \vdots & \vdots & \vdots & \vdots & \vdots \\ k_{N1}^{F\delta} & \dots & k_{Ni}^{F\delta} & \dots & k_{NN}^{F\delta} & k_{N1}^{F\varphi} & \dots & k_{Ni}^{F\varphi} & \dots & k_{NN}^{F\varphi} \\ \vdots & \vdots & \vdots & \vdots & \vdots & \vdots & \vdots & \vdots & \vdots & \vdots \\ k_{11}^{M\delta} & \dots & k_{1i}^{M\delta} & \dots & k_{1N}^{M\delta} & k_{11}^{M\varphi} & \dots & k_{1i}^{M\varphi} & \dots & k_{1N}^{M\varphi} \\ \vdots & \vdots & \vdots & \vdots & \vdots & \vdots & \vdots & \vdots & \vdots & \vdots \\ k_{i1}^{M\delta} & \dots & k_{ii}^{M\delta} & \dots & k_{iN}^{M\delta} & k_{i1}^{M\varphi} & \dots & k_{ii}^{M\varphi} & \dots & k_{iN}^{M\varphi} \\ \vdots & \vdots & \vdots & \vdots & \vdots & \vdots & \vdots & \vdots & \vdots & \vdots \\ k_{N1}^{M\delta} & \dots & k_{Ni}^{M\delta} & \dots & k_{NN}^{M\delta} & k_{N1}^{M\varphi} & \dots & k_{Ni}^{M\varphi} & \dots & k_{NN}^{M\varphi} \end{bmatrix} \begin{Bmatrix} \delta_1 \\ \vdots \\ \delta_i \\ \vdots \\ \delta_N \\ \varphi_1 \\ \vdots \\ \varphi_i \\ \vdots \\ \varphi_N \end{Bmatrix}. \quad (2)$$

Referring to the linear system reported in Eq. (2), the generic term  $k_{ij}$  can be seen as the total horizontal force (moment) on the  $i$ th floor  $F_i$  ( $M_i$ ), if a unitary horizontal displacement (rotation)  $\delta_j$  ( $\varphi_j$ ) is imposed on the  $j$ th floor, whereas all the other floor displacements (rotations) are kept null. Applying this analytical definition, the stiffness matrix reported in Eq. (2) can be totally computed through the following steps: (1) a unitary horizontal displacement (rotation) is imposed to the  $j$ th floor, keeping fixed all the other floors (Fig. 3); (2) the diagonal deformations within the deformed modules are evaluated through geometric considerations; (3) the axial forces in the diagonals are computed, assuming a linear elastic behaviour; (4) the total reaction force (moment) acting on the  $i$ th floor, produced by the axial forces of the diagonals, is calculated. As regards the calculation of reaction floor moments or imposed floor rotations, they are evaluated with respect to the stiffness centroid of the  $j$ th floor, whose x-coordinate is expressed as follows:

$$x_{C,j} = \frac{\sum_{d=1}^{n_i} \frac{E_{d,j} A_{d,j}}{L_{d,j}} x_{d,j}}{\sum_{d=1}^{n_i} \frac{E_{d,j} A_{d,j}}{L_{d,j}}}. \quad (3)$$

Note that the horizontal displacement (rotation) of the  $j$ th floor produces a strain mechanism only in the adjacent modules: therefore, the stiffness submatrices reported in Eq. (1) are tridiagonal.

Now, considering the generic diagonal, included within the  $j$ th module, subjected to the unitary horizontal displacement imposed to the  $j$ th floor, and referring to the parameters shown in Fig. 4a, the

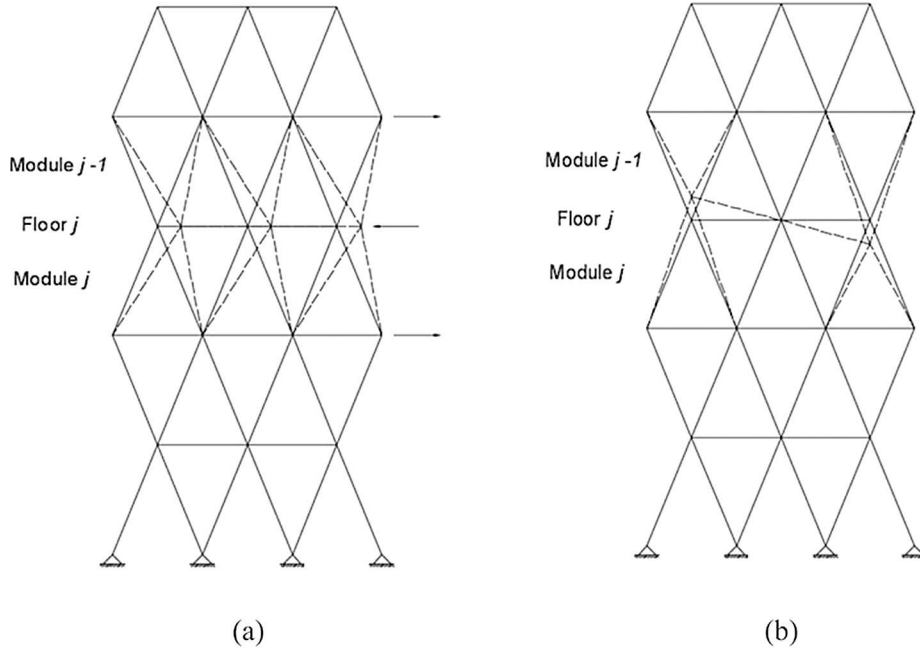


**Fig. 3.** Computation method of the stiffness coefficients: (a) unitary horizontal displacement applied to the  $j$ th floor; (b) unitary rotation applied to the  $j$ th floor.

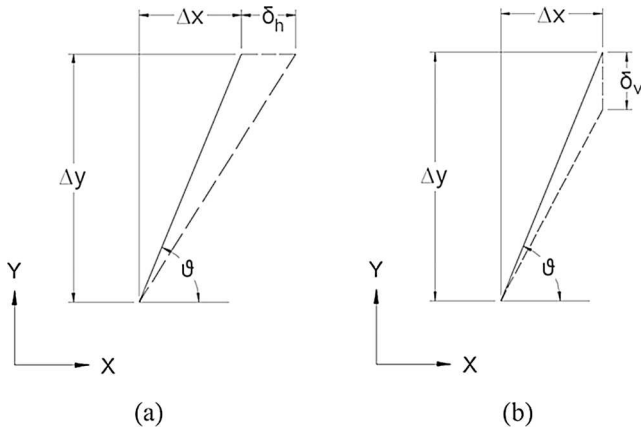


**Fig. 4.** Deformation of the diagonal for (a) horizontal displacements and (b) vertical displacements.

elongation of the diagonal can be expressed as follows:

$$\delta_{diag}^{\delta_h} = \delta_h \cos \vartheta = \delta_h \frac{\Delta x}{L}, \quad (4)$$

where  $\delta_h$  is the imposed horizontal displacement to the  $j$ th floor,  $\vartheta$  is the angle of the diagonal with respect to the horizontal direction,  $L$  is the diagonal length, and  $\Delta x$  and  $\Delta y$  are the projections of the diagonal length with respect to the reference axes.

Taking into account a unitary imposed displacement  $\delta_h$ , and assuming a linear elastic behaviour for the diagonal, the axial force can be written as follows:

$$F_{diag}^{\delta_h} = \frac{EA}{L} \delta_{diag}^{\delta_h} = \frac{EA}{L^2} \Delta x, \quad (5)$$

where  $E$  and  $A$  are respectively the Young's modulus of the diagonal and its cross sectional area. Considering now the diagonal subjected to the vertical displacement generated by the unitary imposed rotation to the  $j$ th floor (Fig. 4b), its elongation can be obtained as follows:

$$\delta_{diag}^{\delta_v} = -\delta_v \sin \vartheta = -\delta_v \frac{\Delta y}{L}, \quad (6)$$

where  $\delta_v$  is calculated by the imposed rotation and depends on the position of the diagonal with respect to the centroid of the floor:

$$\delta_v = \varphi(x - x_c). \quad (7)$$

Therefore, the axial force in the diagonal arising from the unitary rotation of the  $j$ th floor can be obtained as follows:

$$F_{diag}^{\varphi} = \frac{EA}{L} \delta_{diag}^{\delta_v} = -\frac{EA}{L^2} (x - x_c) \Delta y. \quad (8)$$

By decomposing the obtained axial forces along the horizontal and vertical directions, and by computing the total reactive forces in the horizontal directions as well as the reactive moments on each floor, the four stiffness submatrices reported in Eq. (1) can be finally computed.

Below, the complete expressions are reported, where  $n_i$  and  $n_{i-1}$  represent the number of diagonals included respectively in the modules  $i$  and  $i-1$ , and, for each variable, the first subscript refers to the generic diagonal involved in the summation process and the second one refers to the module which the diagonal belongs to. As far as the x-coordinates are concerned,  $x_{d,i-1}$  indicates the x-coordinate of the diagonal  $d$ , included within the  $(i-1)$ th module, referred to the  $i$ th floor, while  $x_{C,i}$  stands for the x-coordinate of the  $i$ th floor centroid.

Matrix  $[K_{FS}]$ :

$$k_{i,i}^{FS} = \sum_{d=1}^{n_{i-1}} E_{d,i-1} A_{d,i-1} \frac{\Delta x_{d,i-1}^2}{L_{d,i-1}^3} + \sum_{d=1}^{n_i} E_{d,i} A_{d,i} \frac{\Delta x_{d,i}^2}{L_{d,i}^3}, \quad (9)$$

$$k_{i-1,i}^{F\delta} = - \sum_{d=1}^{n_{i-1}} E_{d,i-1} A_{d,i-1} \frac{\Delta x_{d,i-1}^2}{L_{d,i-1}^3}, \quad (10)$$

$$k_{i+1,i}^{F\delta} = - \sum_{d=1}^{n_i} E_{d,i} A_{d,i} \frac{\Delta x_{d,i}^2}{L_{d,i}^3}. \quad (11)$$

Matrix  $[K_{F\varphi}]$ :

$$k_{i,i}^{F\varphi} = - \sum_{d=1}^{n_{i-1}} E_{d,i-1} A_{d,i-1} \frac{\Delta x_{d,i-1} \Delta y_{d,i-1}}{L_{d,i-1}^3} (x_{d,i-1,i} - x_{C,i}) - \sum_{d=1}^{n_i} E_{d,i} A_{d,i} \frac{\Delta x_{d,i} \Delta y_{d,i}}{L_{d,i}^3} (x_{d,i,i} - x_{C,i}), \quad (12)$$

$$k_{i-1,i}^{F\varphi} = \sum_{d=1}^{n_{i-1}} E_{d,i-1} A_{d,i-1} \frac{\Delta x_{d,i-1} \Delta y_{d,i-1}}{L_{d,i-1}^3} (x_{d,i-1,i} - x_{C,i}), \quad (13)$$

$$k_{i+1,i}^{F\varphi} = \sum_{d=1}^{n_i} E_{d,i} A_{d,i} \frac{\Delta x_{d,i} \Delta y_{d,i}}{L_{d,i}^3} (x_{d,i,i} - x_{C,i}). \quad (14)$$

Matrix  $[K_{M\delta}]$ :

$$k_{i,i}^{M\delta} = - \sum_{d=1}^{n_{i-1}} E_{d,i-1} A_{d,i-1} \frac{\Delta x_{d,i-1} \Delta y_{d,i-1}}{L_{d,i-1}^3} (x_{d,i-1,i} - x_{C,i}) - \sum_{d=1}^{n_i} E_{d,i} A_{d,i} \frac{\Delta x_{d,i} \Delta y_{d,i}}{L_{d,i}^3} (x_{d,i,i} - x_{C,i}), \quad (15)$$

$$k_{i-1,i}^{M\delta} = \sum_{d=1}^{n_{i-1}} E_{d,i-1} A_{d,i-1} \frac{\Delta x_{d,i-1} \Delta y_{d,i-1}}{L_{d,i-1}^3} (x_{d,i-1,i-1} - x_{C,i-1}), \quad (16)$$

$$k_{i+1,i}^{M\delta} = \sum_{d=1}^{n_i} E_{d,i} A_{d,i} \frac{\Delta x_{d,i} \Delta y_{d,i}}{L_{d,i}^3} (x_{d,i,i+1} - x_{C,i+1}). \quad (17)$$

Matrix  $[K_{M\varphi}]$ :

$$k_{i,i}^{M\varphi} = \sum_{d=1}^{n_{i-1}} E_{d,i-1} A_{d,i-1} \frac{\Delta y_{d,i-1}^2}{L_{d,i-1}^3} (x_{d,i-1,i} - x_{C,i})^2 + \sum_{d=1}^{n_i} E_{d,i} A_{d,i} \frac{\Delta y_{d,i}^2}{L_{d,i}^3} (x_{d,i,i} - x_{C,i})^2, \quad (18)$$

$$k_{i-1,i}^{M\varphi} = - \sum_{d=1}^{n_{i-1}} E_{d,i-1} A_{d,i-1} \frac{\Delta y_{d,i-1}^2}{L_{d,i-1}^3} (x_{d,i-1,i} - x_{C,i})(x_{d,i-1,i-1} - x_{C,i-1}), \quad (19)$$

$$k_{i+1,i}^{M\varphi} = - \sum_{d=1}^{n_i} E_{d,i} A_{d,i} \frac{\Delta y_{d,i}^2}{L_{d,i}^3} (x_{d,i,i} - x_{C,i})(x_{d,i,i+1} - x_{C,i+1}). \quad (20)$$

Thus, by applying Eqs. (9)–(20), the diagrid stiffness matrix reported in Eq. (1) is computed, and the displacements of the structure can be calculated as follows:

$$\begin{Bmatrix} \{\delta\} \\ \{\varphi\} \end{Bmatrix} = \begin{bmatrix} [K_{F\delta}] & [K_{F\varphi}] \\ [K_{M\delta}] & [K_{M\varphi}] \end{bmatrix}^{-1} \begin{Bmatrix} \{F\} \\ \{M\} \end{Bmatrix}. \quad (21)$$

Once the displacements of the structure are known, going backwards to Eqs. (4)–(8), it is possible to compute the axial force in each diagonal included in the  $i$ th module ( $F_{diag,i}$ ) as follows:

$$F_{diag,i} = \frac{E_{d,i} A_{d,i}}{L_{d,i}^2} [\Delta x_{d,i} (\delta_i - \delta_{i+1}) - \Delta y_{d,i} \varphi_i (x_{d,i,i} - x_{C,i}) + \Delta y_{d,i} \varphi_{i+1} (x_{d,i,i+1} - x_{C,i+1})]. \quad (22)$$

Having implemented this procedure into the MatLab environment, the solution of the structural problem is automatically obtained.

### 3.2. Comparison with FEM analysis

In order to evaluate the accuracy of the proposed method, an example of two-dimensional diagrid structural system has been investigated, in order to compare the results provided by the model implemented in MatLab and the results obtained by the Finite Element code Lusas. The geometry of the eight-story structure is shown in Fig. 5. The total height, module height and base dimension are equal to 84 m, 10.5 m and 30 m, respectively. That means that each module comprises three actual floors, but only the floors at the end of each module have been considered. The cross sectional areas of the diagonals are reported

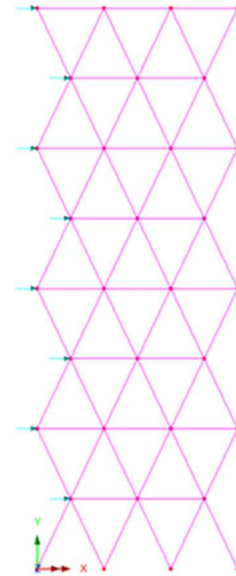


Fig. 5. Geometry of the two-dimensional diagrid finite element model.

**Table 1**  
Diagonals geometrical properties.

Module	Cross Sectional Area [cm <sup>2</sup> ]
1 – 2	280
3 – 4	320
5 – 6	360
7 – 8	400



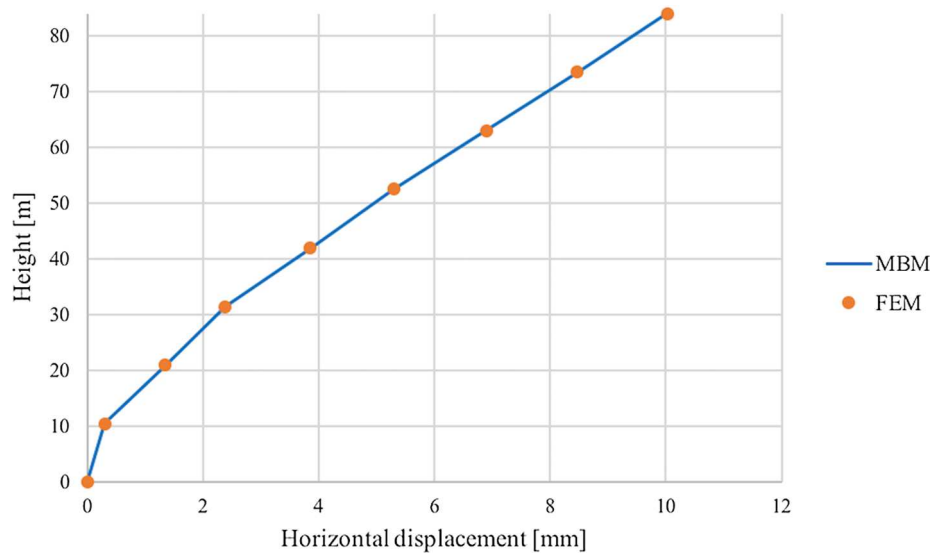


Fig. 6. Horizontal displacements of the modules – 2D example (MBM vs FEM).

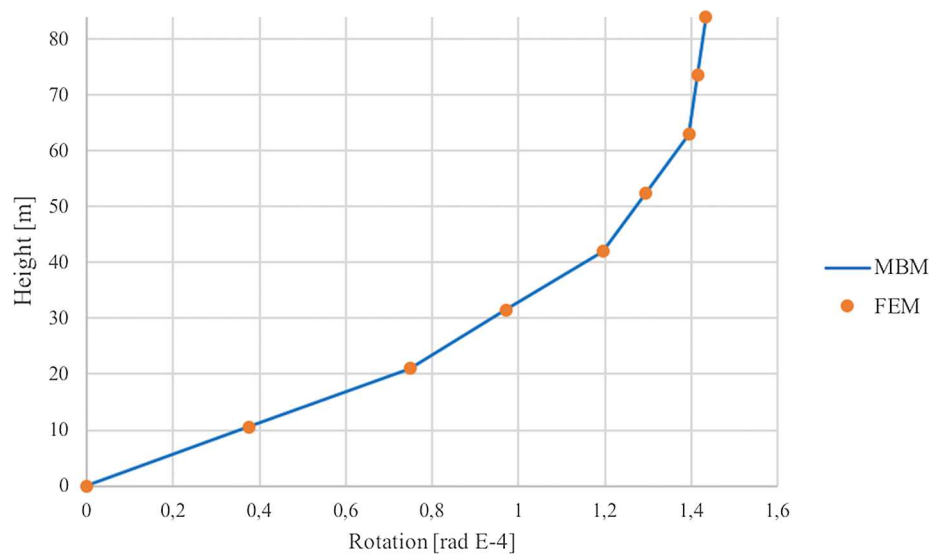


Fig. 7. Out-of-plane rotations of the modules – 2D example (MBM vs FEM).

in Table 1. Note that the diagonals included within the same module have the same geometrical characteristics. The adopted material for the diagonals is assumed to be steel with a Young's Modulus equal to 210 GPa, whereas a greater Modulus has been applied to the horizontal beams in order to take into account the hypothesis of infinitely rigid in-plane floors. As regards the external actions, a system of horizontal forces – each of them equal to 30 kN – has been applied to the floor plans.

In Figs. 6 and 7, the comparison concerning the horizontal

displacements and out-of-plane rotations is reported: the maximum relative error is about 0.2%. Therefore, if the hypothesis of infinitely rigid floors is maintained, the suggested MBM provides consistent results with FEM analysis.

In Figs. 8 and 9, the comparison concerning the axial forces of the six diagonals included respectively within the top and the ground module is reported. As can be seen from the figures the difference between the obtained results is negligible.

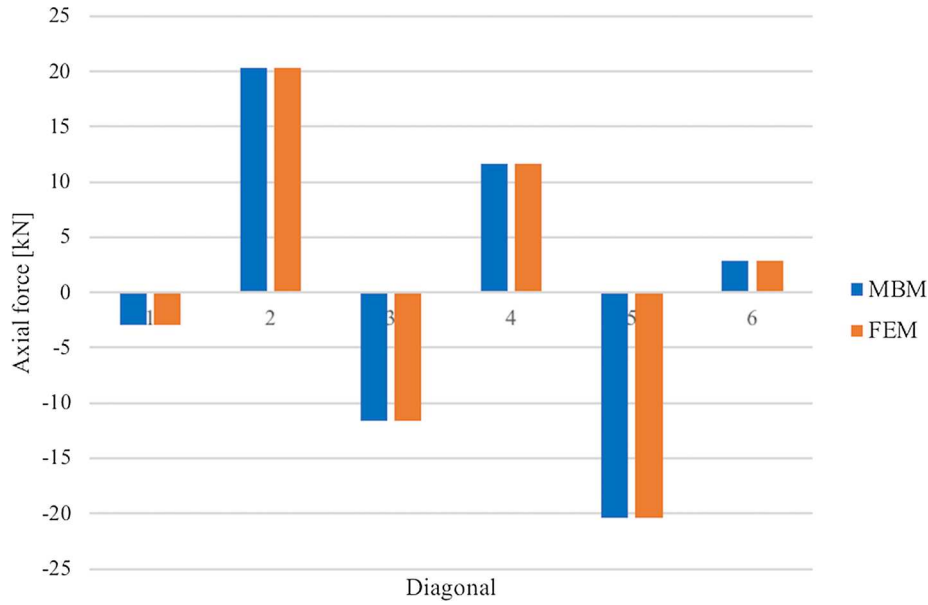


Fig. 8. Axial forces in the diagonals of the top module – 2D example (MBM vs FEM).

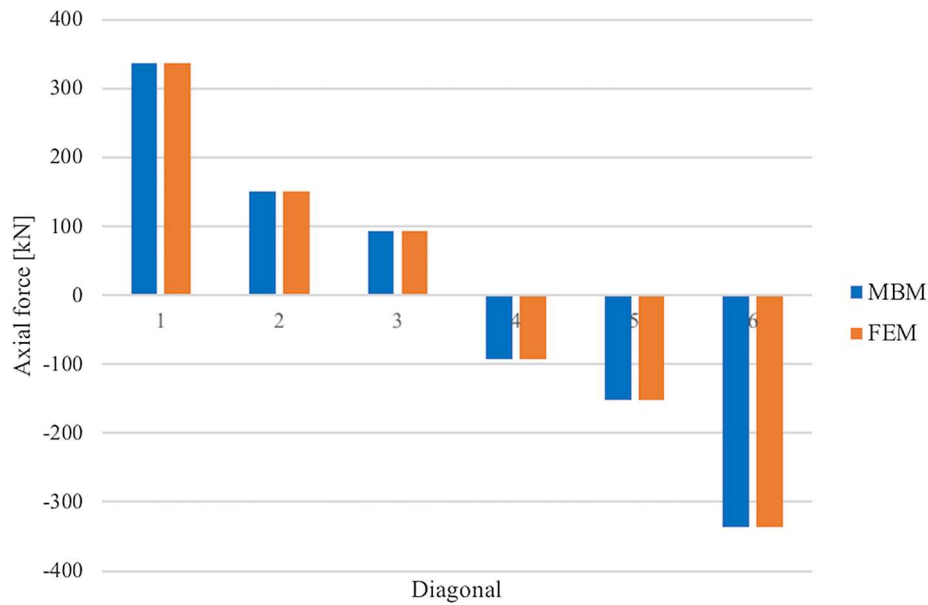


Fig. 9. Axial forces in the diagonals of the ground module – 2D example (MBM vs FEM).

#### 4. Analysis of three-dimensional diagrid systems

##### 4.1. Six-degree-of-freedom per floor model

A generic three-dimensional diagrid structural system is now considered (Fig. 10). It is made up of  $N$  floors (neglecting the inner ones as in Section 3), within a three-dimensional space characterized by an XYZ reference system, where X and Y are the horizontal axes and Z is the vertical one. The main hypotheses are the same taken into account in Section 3: continue and infinitely rigid floors and hinged diagonals. The structure is assumed to be subjected to horizontal floor forces (along X and Y axes), vertical floor forces (along Z axis) and in-plane floor torque moments (around Z axis).

If six degrees of freedom per floor are considered, the structural problem in Eq. (1) can be rewritten by specifying the contributions of the six generalized displacements as follows:

$$\begin{Bmatrix} \{F_x\} \\ \{F_y\} \\ \{M_z\} \\ \{M_x\} \\ \{M_y\} \\ \{F_z\} \end{Bmatrix} = \begin{bmatrix} [K_{F_x\delta_x}] & [K_{F_x\delta_y}] & [K_{F_x\varphi_z}] & [K_{F_x\varphi_x}] & [K_{F_x\varphi_y}] & [K_{F_x\delta_z}] \\ [K_{F_y\delta_x}] & [K_{F_y\delta_y}] & [K_{F_y\varphi_z}] & [K_{F_y\varphi_x}] & [K_{F_y\varphi_y}] & [K_{F_y\delta_z}] \\ [K_{M_z\delta_x}] & [K_{M_z\delta_y}] & [K_{M_z\varphi_z}] & [K_{M_z\varphi_x}] & [K_{M_z\varphi_y}] & [K_{M_z\delta_z}] \\ [K_{M_x\delta_x}] & [K_{M_x\delta_y}] & [K_{M_x\varphi_z}] & [K_{M_x\varphi_x}] & [K_{M_x\varphi_y}] & [K_{M_x\delta_z}] \\ [K_{M_y\delta_x}] & [K_{M_y\delta_y}] & [K_{M_y\varphi_z}] & [K_{M_y\varphi_x}] & [K_{M_y\varphi_y}] & [K_{M_y\delta_z}] \\ [K_{F_z\delta_x}] & [K_{F_z\delta_y}] & [K_{F_z\varphi_z}] & [K_{F_z\varphi_x}] & [K_{F_z\varphi_y}] & [K_{F_z\delta_z}] \end{bmatrix} \begin{Bmatrix} \{\delta_x\} \\ \{\delta_y\} \\ \{\varphi_z\} \\ \{\varphi_x\} \\ \{\varphi_y\} \\ \{\delta_z\} \end{Bmatrix}, \quad (23)$$

where  $\{F_x\}$ ,  $\{F_y\}$  and  $\{F_z\}$  are the  $N$ -vectors containing respectively the floor forces along X, Y and Z axis,  $\{M_z\}$  represents the  $N$ -vector containing the in-plane floor torque moments, while  $\{M_x\}$  and  $\{M_y\}$  are the  $N$ -vectors containing respectively the out-of-plane floor moments along X and Y axes. As for the floors displacements,  $\{\delta_x\}$ ,  $\{\delta_y\}$  and  $\{\delta_z\}$  are the  $N$ -vectors containing respectively the displacements along X, Y and Z axis,  $\{\varphi_z\}$  represents the  $N$ -vector containing the in-plane floor rotations,

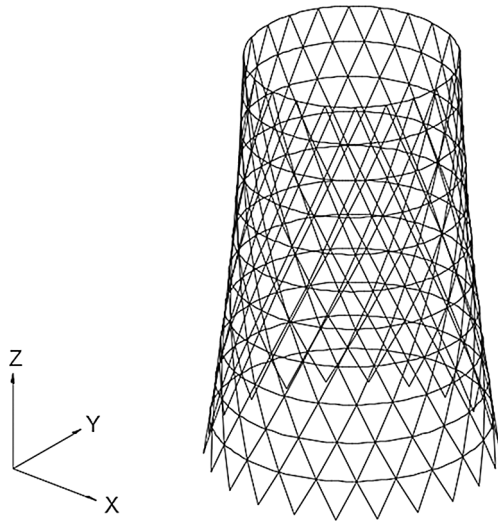


Fig. 10. Three-dimensional diagrid structural system.

while  $\{\varphi_x\}$  and  $\{\varphi_y\}$  are the  $N$ -vectors containing respectively the out-of-plane floor rotations along X and Y axes.

The complete stiffness matrix of the structure ( $6N \times 6N$ ) is presented in Eq. (23), through its partition based on the six degrees of freedom: each submatrix ( $N \times N$ ) represents the stiffness matrix which relates each floor force/moment vector to each displacement/rotation vector. For sake of clarity, in Fig. 11a the conventions about the displacements/rotations are reported.

Each of these matrices can be computed following the same procedure reported in Section 3: (1) a unitary displacement or a unitary rotation is applied to the  $j$ th floor; (2) the deformations and the axial forces of the diagonals included within the deformed modules are computed; (3) the total reactive force or the total reactive moments at the  $i$ th floor is evaluated. Therefore, following the conventions shown in Fig. 11b, it is possible to compute the stiffness coefficients included within the thirty-six submatrices. Once the stiffness matrix of the three-dimensional diagrid system is computed, the structural problem can be automatically solved inverting the linear system reported in Eq. (23). Moreover, known the displacements and the rotations of the rigid floors, it is possible to evaluate the axial forces into the generic diagonals through an equation similar to Eq. (22), but much more complicated because it contains the contributions of all six degrees of freedom.

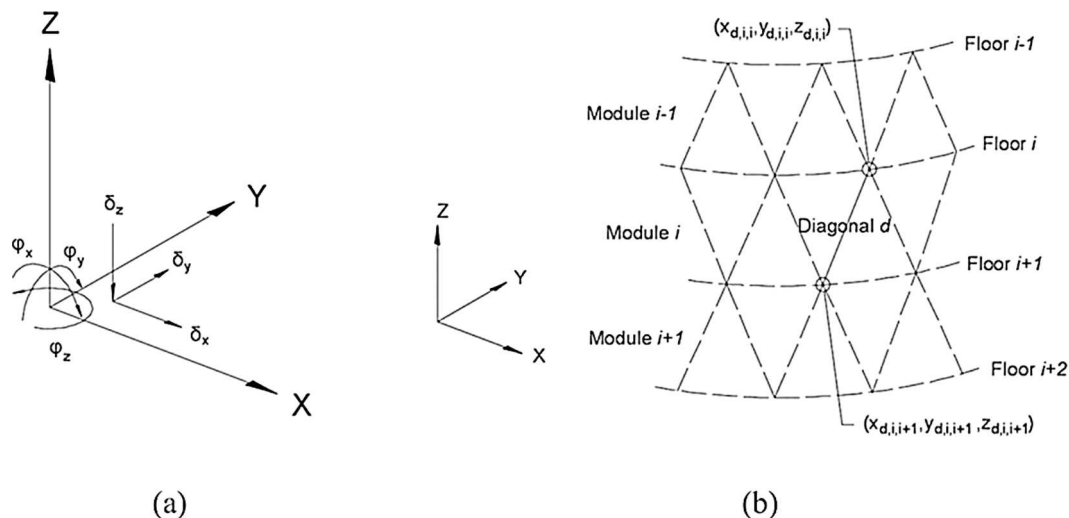


Fig. 11. Conventions for three-dimensional diagrid structure: (a) displacements and rotations of the floors; (b) floors and modules numbering and subscripts of diagonal coordinates.

#### 4.2. Comparison with FEM analysis

The proposed MBM has been applied in order to perform the structural analysis of the Swiss Re Tower (Fig. 1a): the results provided by the suggested model implemented in MatLab have been compared to the FEM analysis executed using the Finite Element code Lusas.

The geometry of the diagrid system is shown in Fig. 12. In agreement with the analysis performed in [12], the top steel-glass dome has not been included within the model because it is considered as a dead load, rather than a structural element. The circular floors present variable dimensions along the elevation: the diameter is equal to 49 m at the ground floor, 30 m at the top floor, and 56 m at the widest point, located at the 20th floor. The structure is made up of 40 floors, with a typical inter-storey height equal to 4.15 m. However, in agreement with the abovementioned hypothesis of neglecting the floors included within

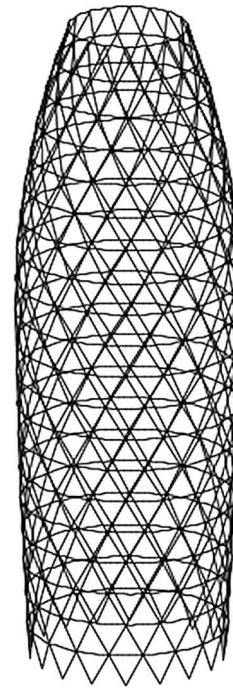


Fig. 12. Geometry of the Swiss Re Tower finite element model.



**Table 2**  
Swiss Re Tower diagonals geometrical properties.

Module	Dimensions <sup>a</sup> [mm]	Area [cm <sup>2</sup> ]	Module	Dimensions <sup>a</sup> [mm]	Area [cm <sup>2</sup> ]
1 – Top level	273 × 12.5	102	11	402 × 27.5	324
2	285 × 14.0	119	12	414 × 29.0	351
3	298 × 15.5	138	13	427 × 30.6	381
4	311 × 17.0	157	14	440 × 32.1	411
5	324 × 18.5	178	15	453 × 33.6	443
6	337 × 20.0	199	16	466 × 35.1	475
7	350 × 21.5	222	17	479 × 36.6	509
8	363 × 23.0	246	18	492 × 38.1	543
9	376 × 24.5	271	19	508 × 40.0	588
10	389 × 26.8	305	20 – Ground level	508 × 40.0	588

<sup>a</sup> Dimensions are referred to CHS sections.

the diagonals modules, since each diagonal extends through two levels, only 20 floors are considered, with a total inter-storey height equal to 8.30 m. Therefore, the total height of the structure is equal to 166 m. The cross sectional areas of the diagonals are reported in Table 2, in agreement with the values adopted in [12]. The adopted material for the diagonals is assumed to be steel with a Young's Modulus equal to 210 GPa. Finally, the following constant actions along the elevation have been considered: unidirectional horizontal floor forces equal to 1500 kN (which correspond approximately to the total wind load evaluated in [12]), downward vertical floor forces equal to 12,000 kN and in-plane torque floor moments equal to 3000 kNm (which take into account an eccentricity of the horizontal forces equal to 2 m).

In Figs. 13–16, the comparison concerning the displacements and rotations is reported: the maximum difference between the results is about 0.3%. In particular, in Figs. 13 and 14 the horizontal

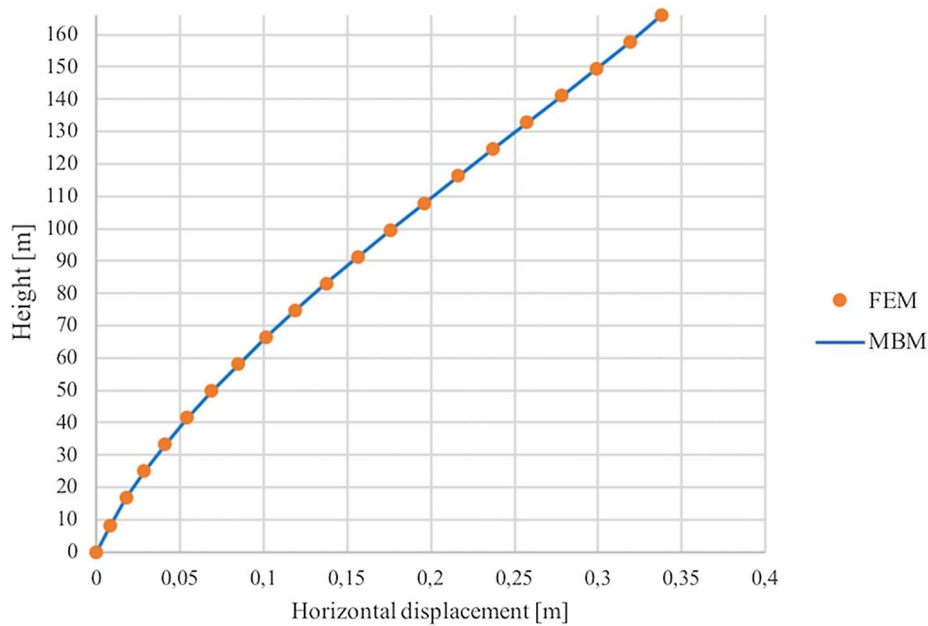


Fig. 13. Horizontal displacements of the modules – Swiss Re Tower (MBM vs FEM).

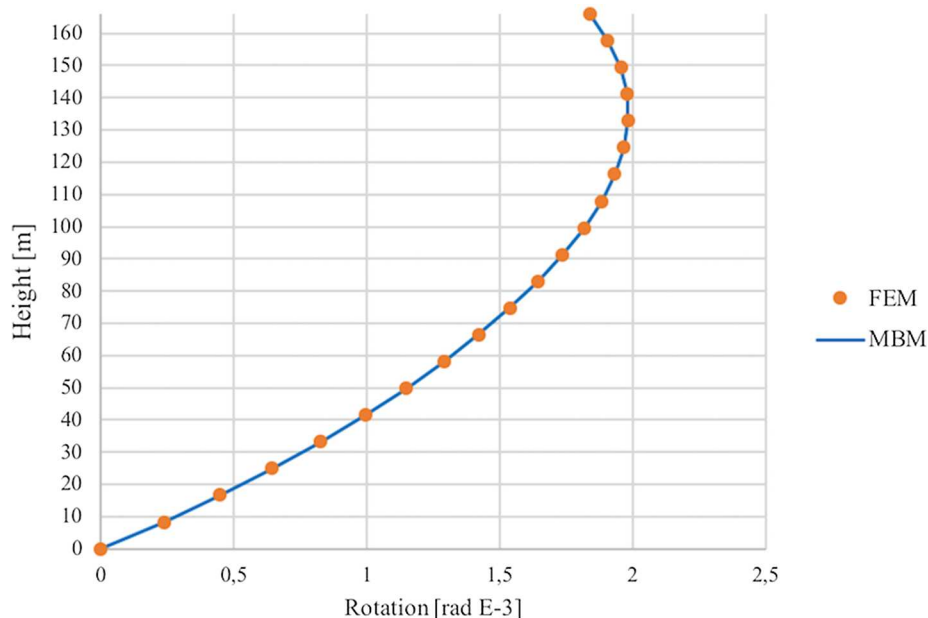


Fig. 14. Out-of-plane rotations of the modules – Swiss Re Tower (MBM vs FEM).

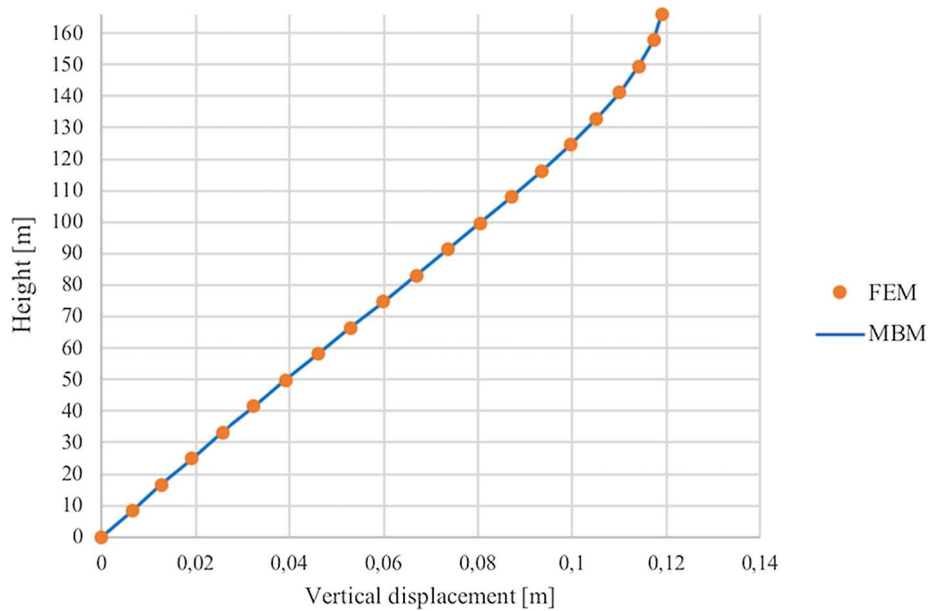


Fig. 15. Vertical displacements of the modules – Swiss Re Tower (MBM vs FEM).

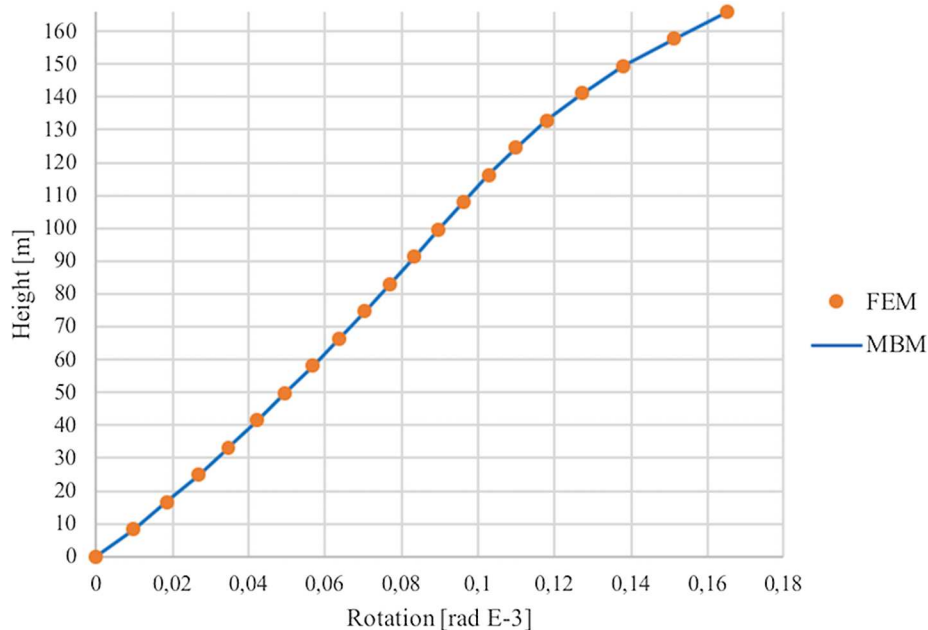


Fig. 16. In-plane torque rotations of the modules – Swiss Re Tower (MBM vs FEM).

displacements and the out-of-plane rotations produced by the horizontal floor forces are reported, and in Fig. 15 the results concerning the vertical displacements produced by the downward vertical floor forces are presented. Finally, in Fig. 16 the results concerning the torque rotations produced by the in-plane torque moments are reported. It is interesting to observe that, as a consequence of the reduction of floor dimensions in the top portion of the structure, the torque rotations increase due to the torque stiffness reduction, whereas a more complex behaviour is exhibited by the out-of-plane rotations.

In Figs. 17 and 18, the comparison concerning the axial forces of the thirty-six diagonals included respectively within the top and the ground module is reported. As the Swiss Re Tower floors are circular, the adopted graphs, already used in [12], are particularly effective for showing the results. Each number reported on the graph border represents one of the thirty-six diagonals included within the circular module, whereas the different concentric circles quantify the axial force

level. Referring to the plans of the shown modules, the horizontal forces are supposed to act from left to right and torque moments are anticlockwise. As can be seen by the obtained results, if the floors are assumed infinitely rigid in-plane, the suggested MBM gives consistent results with classic FEM analysis.

It is worth noting that the linear problem which MBM is based on is characterized by  $6N$  unknowns (i.e. three displacements and three rotations per floor). Otherwise, solving the structural problem through FEM analysis, the number of unknowns is much higher as it includes the displacements of all the nodes defined in the FE model. Therefore, the computational cost required for solving a linear system being more than proportional to the number of unknowns, MBM turns out to be more efficient regarding computational cost. For instance, in the case of Swiss Re Tower, the total number of unknowns is equal to 120 for MBM and it is approximately equal to 1100 for the realized FE model. Therefore, FEM linear problem is almost 10 times bigger compared to MBM one.

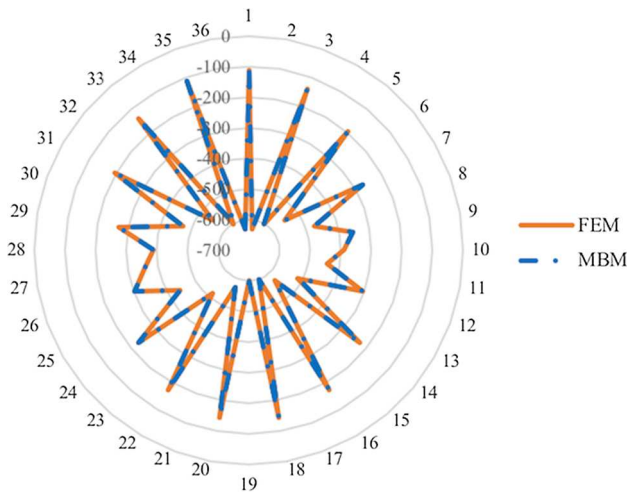


Fig. 17. Axial forces [kN] in the diagonals of the top module – Swiss Re Tower (MBM vs FEM).

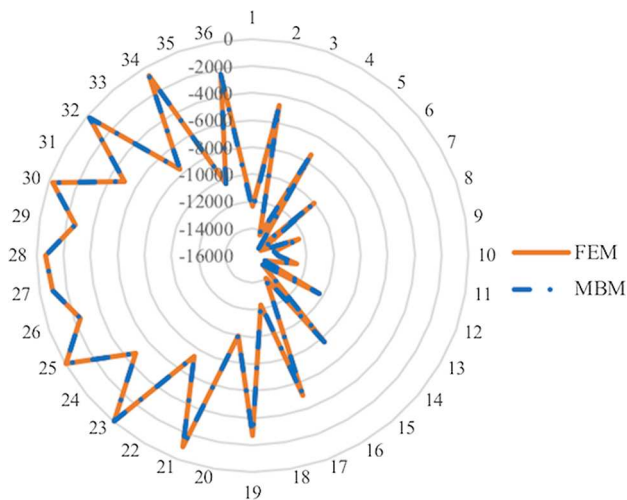


Fig. 18. Axial forces [kN] in the diagonals of the ground module – Swiss Re Tower (MBM vs FEM).

Since the computational cost for solving linear problems is generally proportional to  $n^2$ ,  $n$  being the number of unknowns, the MBM-related computational cost for this kind of problem should be almost 100 times less than the FEM-related one. For sake of completeness, it must however be observed that the modern FE software provide advanced tools for minimizing the computational cost, thus leading to different evaluations in quantitative terms.

## 5. Application within the so called General Algorithm

The General Algorithm was developed in 1985 to study the distribution of lateral actions between different vertical resisting elements, such as shear wall-frames or thin-walled closed and open sections, within a complex three-dimensional civil structure [15]. The Algorithm was then further developed providing a detailed description of the equations used for the calculation process in a static procedure [16–19], also highlighting specific effects, usually secondary in the common structural solutions, but that may be important in tall buildings [20]. Furthermore, another paper on the topic of high-rise structural systems describing the calculation algorithm from a static and dynamic point of view has been published [21].

The main assumptions, which the General Algorithm is based on, are the following ones: (1) generic three-dimensional civil buildings made up of  $N$  floors and  $N_{TOT}$  resisting elements are considered; (2) structural elements are assumed not to be axially deformable; (3) floors are assumed to be infinitely rigid in their own plane; (4) the structure is supposed to be subjected only to horizontal floor forces and in-plane floor torque moments; (5) only three degrees of freedom per floor are considered, two horizontal displacements and one in-plane rotation. Starting from the calculation of the stiffness matrices ( $3N \times 3N$ ) of the resisting elements, the General Algorithm allows to evaluate the distribution matrix, which quantifies the portion of external forces absorbed by each element, according to the following equation [15]:

$$\{F_i\} = [K_i][K]^{-1}\{F\} = [K_i] \left( \sum_{i=1}^{N_{TOT}} [K_i] \right)^{-1} \{F\}. \quad (24)$$

In any event, it is important to note how the suggested MBM for the analysis of three-dimensional diagrid systems, although it has been designed to analyse the mechanical behaviour of a diagrid structure considered as acting alone, can also follow the above mentioned

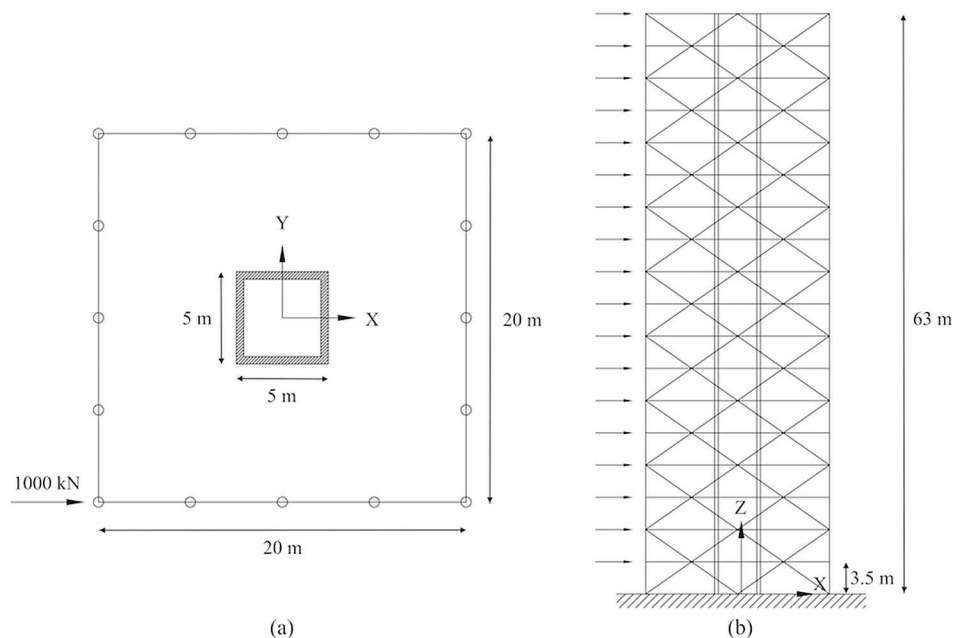


Fig. 19. Diagrid system coupled with central core: (a) top view; (b) side view.

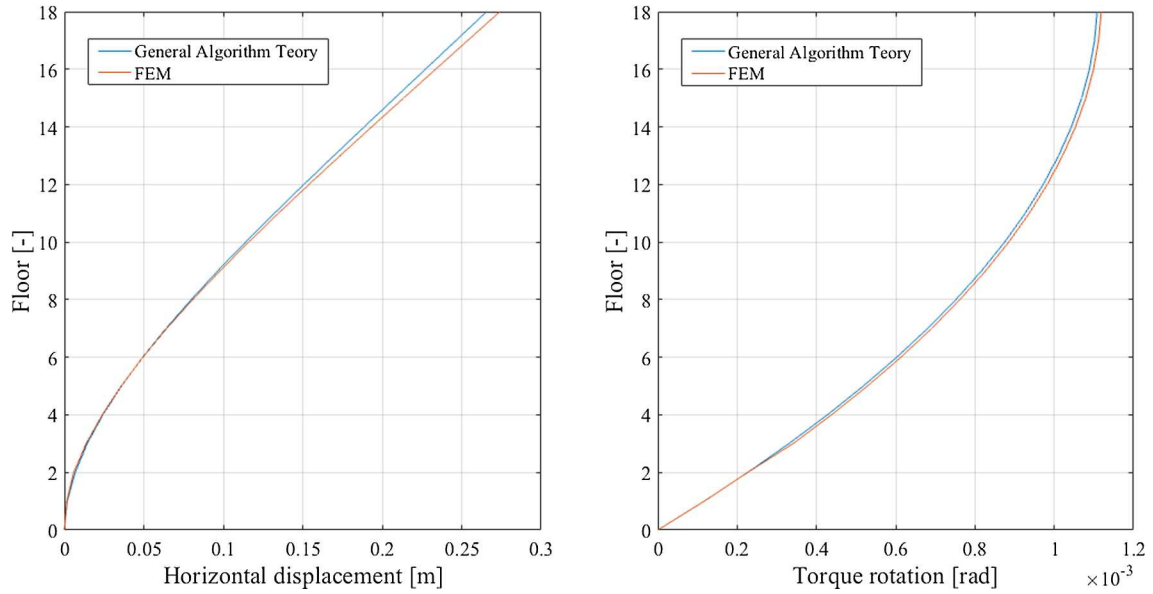


Fig. 20. Diagrid system coupled with central core: (a) horizontal displacements; (b) torque rotations.

assumptions of the General Algorithm. This hypothesis is valid if additive considerations are applied to the MBM as follows.

The MBM allows to compute the stiffness matrix of the diagrid system ( $6N \times 6N$ ), as reported in Eq. (23). Therefore, in order to make the model compatible with all the General Algorithm hypotheses, it is sufficient to neglect the presence of vertical forces and to condense the contributions given by the out-of-plane rotations. In particular, the linear system reported in Eq. (23) can be rewritten separating the parts referring to horizontal displacements  $\{\delta_H\}$  (made up of  $\{\delta_x\}$ ,  $\{\delta_y\}$  and  $\{\delta_z\}$ ) and horizontal forces  $\{F_H\}$  ( $\{F_x\}$ ,  $\{F_y\}$  and  $\{M_z\}$ ) from those referring to vertical displacements  $\{\delta_V\}$  ( $\{\varphi_x\}$ ,  $\{\varphi_y\}$  and  $\{\delta_z\}$ ) and vertical forces  $\{F_V\}$  ( $\{M_x\}$ ,  $\{M_y\}$  and  $\{F_z\}$ ) as follows:

$$\begin{Bmatrix} \{F_H\} \\ \{F_V\} \end{Bmatrix} = \begin{bmatrix} [K_{HH}] & [K_{HV}] \\ [K_{VH}] & [K_{VV}] \end{bmatrix} \begin{Bmatrix} \{\delta_H\} \\ \{\delta_V\} \end{Bmatrix}. \quad (25)$$

In agreement with the General Algorithm, if the structure is supposed to be only subjected to horizontal forces and in-plane torque moments, and if only three degrees of freedom per floor in the

horizontal plane are considered, Eq. (25) can be simplified as follows:

$$\{F_H\} = ([K_{HH}] - [K_{HV}][K_{VV}]^{-1}[K_{VH}])\{\delta_H\} = [K_{HH}]^*\{\delta_H\}. \quad (26)$$

With these simplifications, Eq. (26) satisfies all the above mentioned hypotheses; therefore, the diagrid stiffness matrix  $[K_{HH}]^*$  ( $3N \times 3N$ ) can be inserted within the General Algorithm, in order to study the stiffness interaction between diagrid elements and other structural members.

An application of the MBM is thus proposed in order to evaluate the distribution of lateral actions between an external diagrid system and a central core, according to the General Algorithm theory. The plan of the building is shown in Fig. 19a: it is made up of a  $20\text{ m} \times 20\text{ m}$  square diagrid system and a  $5\text{ m} \times 5\text{ m}$  central concrete core. The total height of the building is equal to 63 m, being composed by 18 modules and 18 floors with an inter-story height equal to 3.5 m (Fig. 19b). The concrete core is 40 cm thick and is characterized by a Young's Modulus of 30 GPa. Whereas, all the diagrid diagonals are made of steel ( $E = 210\text{ GPa}$ ) and  $508 \times 25.0\text{ mm}$  CHS sections are assigned ( $A = 380\text{ cm}^2$ ). According to the described geometry, the elevation angle of each diagonal

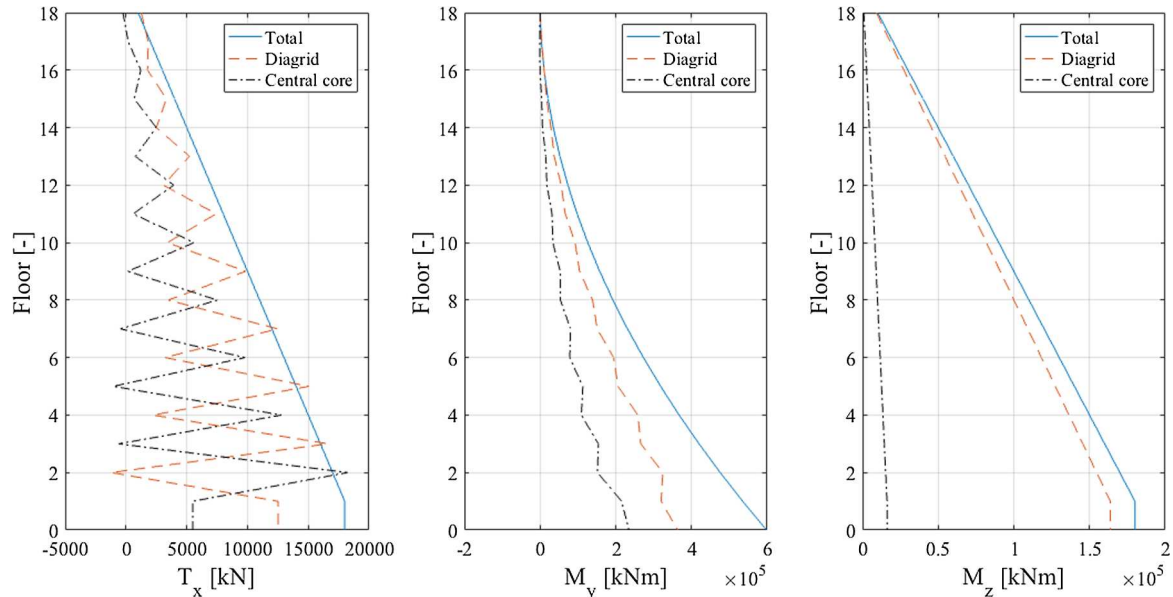


Fig. 21. Diagrid system coupled with central core: (a) shear; (b) bending moment; (c) torque moment.

is equal to  $35^\circ$ . The structure is subject to horizontal floor forces which are constant along the elevation and equal to 1000 kN. These are applied with an eccentricity of 10 m with respect to the centroid of the building (Fig. 19a).

In Fig. 20 the horizontal displacements and torque rotations of the buildings are shown, according to the General Algorithm theory as well as to FEM results. The maximum relative difference are 3.0% and 0.9% for the top horizontal displacement and the top torque rotation respectively, thus confirming the validity of the MBM associated to the General Algorithm. Moreover, shear values as well as bending and torque moments acting on the structure floors are shown in Fig. 21.

It is interesting to observe how these static features distribute between the two resistant elements. About the 70% of the base shear is absorbed by the diagrid, whereas about the 30% is withstood by the concrete core, although a remarkable oscillating trend is noticeable along the elevation of the building. In the same way, about the 60% of the base bending moment is absorbed by the diagrid and the 40% by the central core. The oscillation is mainly due to the fact that the diagrid structure exhibits a significant variation of its flexural stiffness along the height of the building. Indeed the resistance to the out-of-plane rotations of the diagrid is not uniform since, as can be noticed from Fig. 19b referring to the vertical façades, the lever arm of the most external diagonals changes for different floors. This strongly affects the variation of the diagrid lateral stiffness. Such oscillation has an impact on the distribution of the lateral actions, especially when the diagrid is coupled to the central concrete core, which conversely exhibits a uniform stiffness.

Regarding the torque moments produced by the eccentricity of the horizontal forces, they are withstood by the diagrid for the 91%, whereas the concrete core absorbs only the 9%. It is clear that, by changing the structural features such as the thickness of the central core, the inclination angles and cross sectional areas of the diagrid diagonals, different distributions may be observed. Thus, optimization processes may be conducted in order to find the optimal configuration to minimize the building displacements and the forces within the elements, while reducing the amount of material. From the proposed example, it is clear that the MBM, as far as subject to some restrictive hypotheses, may become a powerful tool to analyse complex spatial structures.

## 6. Conclusions

Dia-grid structural systems are probably going to be one of the most exploited solutions for realizing high-rise buildings, because of their mechanical behaviour and capability to provide impressive freeform structures. The present paper provides a matrix-based method (MBM), based on the direct definition of the diagrid stiffness matrix, for the structural analysis of generic diagrid systems. The procedure differs both from the methodologies reported in [6,13], which suggest analytical hand calculation methods for evaluating only shear and bending stiffness of diagrid structures, and from Finite Element Method, which is based on the assemblage procedure of local sub-matrices. The MBM has then been applied to the analysis of two-dimensional and three-dimensional diagrid systems. In particular, the analysis concerning the

Swiss Re Tower in London has been performed and the comparison with FEM results confirmed the validity of the proposed MBM. Moreover, in order to study the distribution of lateral actions between several resisting elements within a complex three-dimensional building, it has been shown that the proposed MBM can be inserted into the General Algorithm, considering a reduced three-degree-of-freedom per floor model. In order to show the capabilities of MBM associated to the General Algorithm theory, an example has been proposed to evaluate the distribution of lateral actions between an external steel diagrid system and a central concrete core. In future research efforts, the proposed method will be also extended in order to consider both geometrical and material nonlinearities, which may be crucial for this kind of structures.

## References

- [1] Lee K, Loo Y, Guan H. Simple analysis of framed-tube structures with multiple internal tubes. *J Struct Eng* 2001;127:450–60.
- [2] Pekau OA, Lin L, Zielinski ZA. Static and dynamic analysis of tall tube-in-tube structures by finite story method. *Eng Struct* 1996;18:515–27.
- [3] Ali MM, Moon KS. Structural developments in tall buildings: current trends and future prospects. *Arch Sci Rev* 2007;50:205–23.
- [4] Asadi E, Adeli H. Dia-grid: an innovative, sustainable, and efficient structural system. *Struct Des Tall Special Build* 2017;26:e1358.
- [5] Korsavi S, Maqhareh MR. The evolutionary process of diagrid structure towards architectural, structural and sustainability concepts: reviewing case studies. *J Arch Eng Technol* 2014;3:121.
- [6] Moon KS, Connor JJ, Fernandez JE. Dia-grid structural systems for tall buildings: characteristics and methodology for preliminary design. *Struct Des Tall Special Build* 2007;16:205–30.
- [7] Moon KS. Dia-grid structures for complex-shaped tall buildings. *Proc Eng* 2011;14:1343–50.
- [8] Moon KS. Optimal grid geometry of diagrid structures for tall buildings. *Arch Sci Rev* 2008;51:239–51.
- [9] Zhang C, Zhao F, Liu Y. Dia-grid tube structures composed of straight diagonals with gradually varying angles. *Struct Des Tall Special Build* 2012;21:283–95.
- [10] Zhao F, Zhang C. Diagonal arrangements of diagrid tube structures for preliminary design. *Struct Des Tall Special Build* 2015;24:159–75.
- [11] Angelucci G, Mollaioli F. Dia-grid structural systems for tall buildings: changing pattern configuration through topological assessments. *Struct Des Tall Special Build* 2017;26:e1396.
- [12] Mele E, Toreno M, Brandonisio G, De Luca A. Dia-grid structures for tall buildings: case studies and design considerations. *Struct Des Tall Special Build* 2014;23:124–45.
- [13] Liu C, Ma K. Calculation model of the lateral stiffness of high-rise diagrid tube structures based on the modular method. *Struct Des Tall Special Build* 2017;26:e1333.
- [14] Munro D. Swiss Re's Building, London. *Nyheter om stålbyggnad* 2004;3:36–43.
- [15] Carpinteri A. An. Carpinteri. Lateral loading distribution between the elements of three-dimensional civil structure. *Comput Struct* 1985;21:563–80.
- [16] Carpinteri A, Lacidogna G, Puzzi S. A global approach for three-dimensional analysis of tall buildings. *Struct Des Tall Special Build* 2010;19:518–36.
- [17] Carpinteri A, Corrado M, Lacidogna G, Cammarano S. Lateral load effects on tall shear wall structures of different height. *Struct Eng Mech* 2012;41:313–37.
- [18] Carpinteri A, Lacidogna G, Cammarano S. Structural analysis of high-rise buildings under horizontal loads: a study on the Intesa Sanpaolo Tower in Turin. *Eng Struct* 2013;56:1362–71.
- [19] Carpinteri A, Lacidogna G, Cammarano S. Conceptual design of tall and unconventionally shaped structures: an handy analytical method. *Adv Struct Eng* 2014;17:767–83.
- [20] Lacidogna G. Tall buildings: secondary effects on the structural behaviour. *Struct Build* 2017;170:391–405.
- [21] Carpinteri A, Lacidogna G, Nitti G. Open and closed shear-walls in high-rise structural systems: static and dynamic analysis. *Curved Layered Struct* 2016;3:154–71.